ATLAS Silicon Microstrip Semiconductor Tracker (SCT)

Y.Unno[a], representing the ATLAS SCT collaboration[1]

[a]KEK, Oho 1-1, Tsukuba, Ibaraki 305-0801, Japan

Abstract

Silicon microstrip semiconductor tracking system (SCT) will be in operation in the ATLAS detector in the large hadron collider (LHC) at CERN. Challenging issues in the SCT are the radiation tolerance to the fluence of $2x10^{14}$ 1-MeV-neutron-equivalent particles/cm^2 at the designed luminosity of $1x10^{34}$ cm^{-2}/s of the proton-proton collisions and the speed of electronics to identify the crossing bunches at 25 ns. The developments and the status of the SCT are presented from the point of view of these issues. Series production of the SCT will start in the year of 2000 and the SCT will be installed into the ATLAS detector in the year of 2003-2004.

I. Introduction

The large hadron collider (LHC) is under construction at CERN, using the existing LEP tunnel of 27 km circumference, in order to accelerate protons to 7 TeV and to make head-on collisions at the center-of-mass energy of 14 TeV with a luminosity of 10^{34} cm^{-2}s^{-1}[1]. The ATLAS detector, one of the two major general purpose detectors in LHC, was approved as an experiment in 1994 and is planned to be in operation in 2005 [2]. Its tracking detector near the interaction point, the inner detector, was approved to proceed for construction in 1997 [3].

The inner detector tracks charged particles inside a solenoidal magnet, identifies particle trajectories and measures momentum in the magnetic field. Required precision in the spatial resolution, radiation tolerance, and particle separation have demanded to use semiconductor devices in the inner part and gas-drift chambers with transition radiation capability (TRT) in the outer part. The semiconductor devices are further split into the Silicon pixel devices (Pixel) in the inner-most and the Silicon microstrip devices (SCT) in the middle part between the Pixel and the TRT.

The issues, the status of developments, and the schedule of the SCT are described based on the development in the barrel section of the tracker.

II. Detector overview

A. ATLAS

An overview of full ATLAS detector is shown in Figure 1. The full detector is 22 m high, 46 m long, and weighs 7000 tons which comprises approximately of the inner detector of 4 t, Liq.Ar calorimeter 700 t, Tile calorimeter 4000 t, Muon chambers 500 t, the solenoid 3 t, Air-core toroids 1300 t, and the supports 500 t. The concept of the detector is to measure (with major goals in parenthesis)

1. the momentum of muons precisely in the outside of the calorimeter with the magnetic field generated by the air-core superconducting toroidal magnets (for measuring the Higgs particle decays, H $\rightarrow$ $\mu\mu\mu\mu$),
2. the electromagnetic particles, such as electrons, positrons, and γ's, precisely with a radiation tolerant calorimeter (for measuring H $\rightarrow$ $\gamma\gamma$),
3. the missing hadronic energy with a hadronic calorimeter (for identifying SUSY particle decays, SUSY $\rightarrow$ normal particles + missing energy), and
4. the charged particles, inside the calorimeter, with a solenoidal magnetic field (for identifying b- and tau- particles, and event topologies).

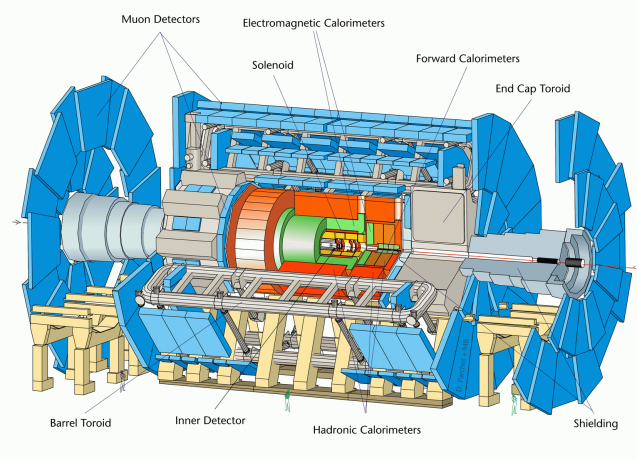

Figure 1: Overview of ATLAS detector at LHC

B. Inner detector

Although tiny compared to the full ATLAS detector, the inner detector is still large and complex: 2.3 m in diameter, 7 m in length. The detection elements are, from the interaction point, Pixel detectors (3 layers), Semiconductor tracker (SCT) which is based on Silicon microstrip detectors (4 layers), and Transi-

[1]Univ. Melbourne, Univ. Sydney, Australia; Acad. Scie. Czech Rep., Czech Tech. Univ., Charles Univ., Czech; Univ. Freiburg, MPI Munich, Germany; NIKHEF, Holland; Hiroshima Univ., KEK, Kyoto Univ. Edu., Okayama Univ., Univ. Tsukuba, Japan; Univ. Bergen, Univ. Oslo, Norway; INP Cracow, FPNT Cracow, Poland; Moscow State Univ., IHEP Protovino, Russia; Univ. Ljubljana, Slovenia; Univ. Valencia, Spain; Univ. Uppsala, Sweden; Univ. Bern, CERN, Univ. Geneva, Switzerland; Univ. Birmingham, Univ. Cambridge, Univ. Glasgow, Lancaster Univ., Univ. Liverpool, Univ. Manchester, Oxford Univ., QMW, RAL, Sheffield Univ., UCL, UK; Univ. California-Irvine, LBNL, Univ. California-Santa Cruz, Univ. Wisconsin, US

tion Radiation Tracker (TRT) based on the straw drift tubes with interleaved transition radiator made of polypropylene foils (64 layers or more). The layout is shown in Figure 2.

The function of the inner detector is to track the charged particles in the 2 Tesla solenoidal magnetic field. The major issues in the tracking are:

1. Precision measurement of positions, in order to identify the trajectories, measure the momenta, and identify the charges of particles, where the precision is defined to identify the charges up to 500 GeV/c,
2. Enhanced electron identification,
3. Speed of electronics, in order to tag the bunches which crosses every 25 ns,
4. Radiation tolerance to the fluence of charged and neutral particles liberated from the primary interactions and from the walls and the calorimeters, in order to survive for 10 years of operation,
5. Amount of materials, which scatters the particles and introduces inaccuracy in the measured momentum and energy, and
6. Cost.

The layout of the inner detector is the result of optimization of the ATLAS collaboration. The position resolutions in the $r\phi$ direction are 12 μm / layer in Pixel, 16 μm / layer in SCT, and 28 μm / 36 straws per track.

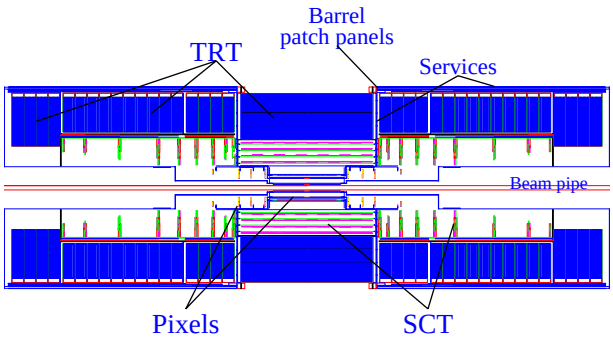

Figure 2: Layout of the inner detector

C. SCT (Silicon microstrip semiconductor tracker)

SCT, covering the pseudo-rapidity range of -2.5 to +2.5 with four layers of cylinders in the barrel and a pair of 9 layers of disks in the forward section, requires an area of 61 m^2 of Silicon microstrip sensors. Precision of the SCT is achieved with a strip pitch of 80 μm, a pair of sensors being arranged to have a small stereo angle of 40 mrad in a layer, which results in a resolution of the pair,

$$\sigma(r\phi) \sim (80\mu m)/(\sqrt{12})/(\sqrt{2}) = 16\mu m \quad .$$

Optimization in cost and the double-occupancy in a strip resulted in using two near-square sensors daisy-chained to form a strip length of 12 cm. One microstrip sensor has a size of 63.6 mm (width) x 64.0 mm (length) with the strip length of 62.0 mm, which is a maximum size made out of a 4-inch Silicon wafer. The layout of the sensor is shown in Figure 3. A number of fiducial marks are implemented in the surrounding edges for alignment and identification. There are 768 readout strips, with integrated AC-coupled readout metals, in the sensor.

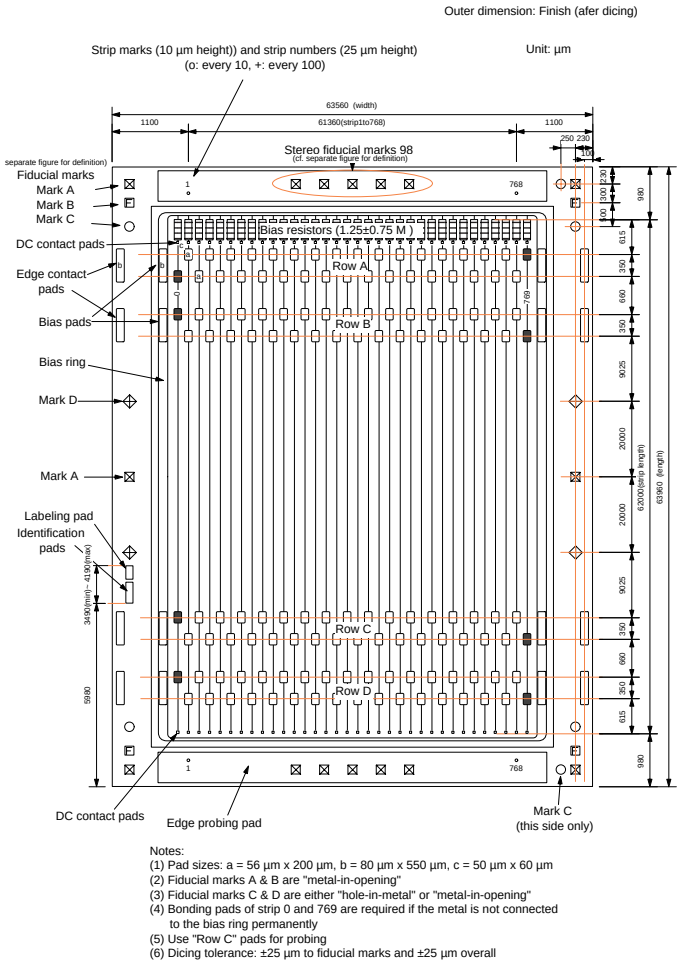

Figure 3: Layout of the Silicon microstrip sensor in the barrel section of the SCT

D. Radiation tolerance

At the designed luminosity of $1x10^{34}$ $cm^{-2}s^{-1}$ of the proton-proton collisions, a yearly fluence of charged and neutral particles has been estimated. The fluence, expressed as the fluence of neutrons of 1 MeV kinetic energy giving equivalent non-ionizing damages, is shown in Figure 4. The expectation has a systematic uncertainty of 50% due to the uncertainties in the proton-proton cross sections, etc. The cumulative fluence over 10 years can be calculated by assuming the LHC operation of a low luminosity of $1x10^{33}$ $cm^{-2}s^{-1}$ in the first 3 years and a high

luminosity of $1x10^{34}$ $cm^{-2}s^{-1}$ in the rest of 7 years.

At the inner-most radius of the barrel section of the SCT, r=30 cm, the yearly fluence is ~$1.8x10^{13}$ n/cm^2 /yr/ L=10^{34}. In 10 years, with including the 50% uncertainty in the fluence, the 1-MeV neutron equivalent fluence is ~$2x10^{14}$ n/cm^2. Since the damage by protons of more than several GeV/c is about 60 to 70% of the damage by 1-MeV neutrons, the fluence of protons of ~$3x10^{14}$ p/cm^2 must be considered in testing the radiation tolerance with protons.

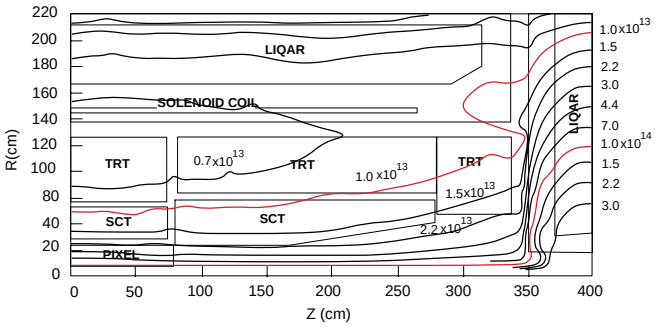

Figure 4: Yearly fluence of charged and neutral particles, translated into the 1-MeV neutrons, in the inner detector

III. Development and Status of SCT

A. Radiation-hard Silicon microstrip sensor

The SCT collaboration has been involved in the development of the radiation-hard Silicon microstrip sensors for years. Development in understanding of the radiation damage, development in the sensor designs, and understanding of the cost, has lead the collaboration to reach the final choice.

In an historical order, the single-sided n-strip readout in the n-bulk Silicon, the n-in-n sensor, was chosen between the n-in-n and the double-sided sensors. The basic arguments for the choice were the understanding of the full depletion voltage being over 300 V for a 300 μm thick Silicon wafers after the SCT fluence, mutation of bulk from the n- to the p-type, and a high voltage to the integrated AC coupling or floating one side of the readout electronics in the double-side sensors. The n-in-n single-sided sensor provides operation of null voltage to the AC coupling and capability of partially depleted operation since the p-n junction is in the strip side after the type inversion. Although the n-in-n sensors have a good operational margin in the radiation tolerance, it has required a double-side process.

The Silicon microstrip sensors commonly used are the p-strip readout in the n-bulk Silicon, the p-in-n sensors. The p-in-n sensor has cost advantage over the n-in-n sensor since the backside process is simpler. Development in understanding of the radiation damage to the p-in-n sensor and development in the structures withstanding the high bias voltage and the high electric field around the strip edges showed that the damaged p-in-n sensors still works after the SCT fluence. Charge collection measurements in a beamtest and with a beta-source, noise measurement, etc., have confirmed the performance of the p-in-n sensors to satisfy the requirement of SCT. The SCT collaboration has finally decided the p-in-n sensor for its choice.

An example of the leakage current characteristics of the latest design, the wide-metal p-in-n sensor [4], is shown in Figure 5. Ten sensors were irradiated for $3x10^{14}$ protons/cm^2, annealed to be equivalent after the 10 years of operation [5], and measured at -18 °C. The figure shows 6 samples. The leakage currents are, although gradually increasing, smooth up to the bias voltage of 500 V. All 10 samples irradiated showed the similar characteristics.

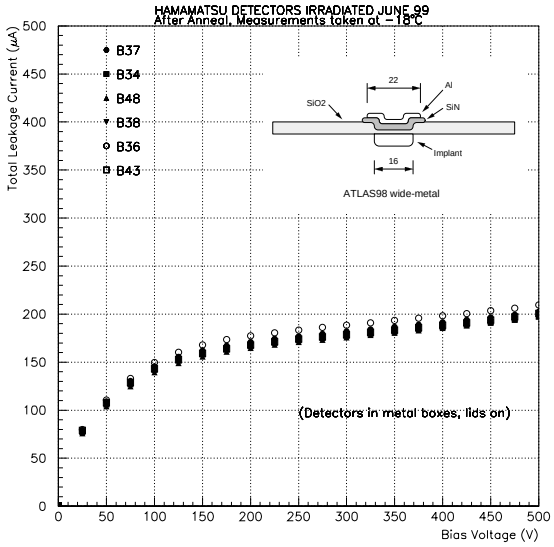

Figure 5: Leakage current vs bias voltage of the wide-metal design of the p-in-n sensor of the SCT, after $3x10^{14}$ protons/cm^2 damage

The inset of the Figure 5 shows the strip structure of the wide-metal sensor. The passivation layer made of SiO_2 over the top surface is not shown in the figure. The strip edge is where the electric field concentrates. If the electric field strength exceeds the avalanche breakdown voltage of the material, it will generate the leakage current and electric noises: the onset of the microdischarge [6]. A tiny defect at the edge also makes the field concentrate and initiates the breakdown much earlier than the global one. The SCT operates the implant and the metal strips in the same potential. In this case, when the metal is wider than the implant strip, the concentration of the electric field is at the edge of the wider electrode which is inside the SiO_2 whose avalanche breakdown voltage is an order larger than that of Silicon. The wider electrode over the implant strip is also known as the “field plate”.

Other characteristics confirmed in the irradiated samples

were: long-term stability of leakage current over 24 hrs., which had no surprise; number of shorts in the AC couplings, which was also excellent. The number of shorts in the samples is summarized in Table 1. A single sensor has 768 strips and an average fraction of the shorts was slightly above 0.2%, even after applying the 100 V voltage.

Table 1.
Number of shorts in AC coupling

	Irradiation	Before	After (10V)	After (100V)
Sample 1	April 99	0	0	0
Sample 2	April 99	0	0	2
Sample 3	April 99	0	0	1
Sample 4	June 99	0	1	1
Sample 5	June 99	0	3	3
Sample 6	June 99	1	1	3
Average fraction		0.02%	0.11%	0.22%

B. Silicon microstrip sensor production

One geometry of Silicon microstrip sensor is enough to cover the cylindrical geometry in the barrel region of the SCT efficiently, while 5 wedge geometries of sensors are required for the disk geometry in the forward region. SCT has chosen a thinner sensor, 260 μm, in the inner-most part of the barrel and the forward, and a standard but slightly thinner, 285 μm, sensors for the rest of layers, in order reduce the depletion voltage. The sensor mnemonics, thickness, and quantity are listed in Table 2. Production of 19,440 sensors are shared by Hamamatsu photonics, SINTEF, CiS, and CSEM. Pre-series production of 5% is to be evaluated by Aug. 2000 and full production to complete by the fall of 2002.

Table 2
Number of Silicon microstrip sensors in the SCT including 20% spares

Barrel		10,560
B1	260 μm	1,920
B2	285 μm	8,640
Forward		8,880
W12	260 μm	1,000
W21	285 μm	1,400
W22	285 μm	1,600
W31	285 μm	2,340
W32	285 μm	2,340

C. Readout electronics

Another challenging area in the SCT is the readout electronics which is put next to the sensors. The architecture of choice is the one threshold readout, called as “binary” readout, for simplicity and cost. The major goals to the electronics are:

1. Signal-to-noise ratio > 12, with the noise < 1500 e,
2. Speed for tagging the 25 ns bunch, which sets the time walk < 16 ns,
3. Double pulse separation, < 50 ns, for minimizing the dead time,
4. Threshold uniformity < 4% (1 sigma) for assuring low noise occupancy,
5. Stability of the fully-loaded module, and
6. Radiation tolerance.

A schematics of the functionality of the front-end electronics is shown in Figure 6. A channel is a chain of two blocks: the first block of amplification, integration, uni-polar shaping, and discrimination, and the second block of buffering the on/off signals in a memory of 132 depth, until the readout trigger comes, and a readout buffer. A chip is made of 128 channels and control sections. The control sections receive the clock, commands, and readout triggers, and also set the voltages and currents for the threshold and front-end transistors. The buffers and readout circuitries are clocked at the same frequency of the LHC, 40 MHz.

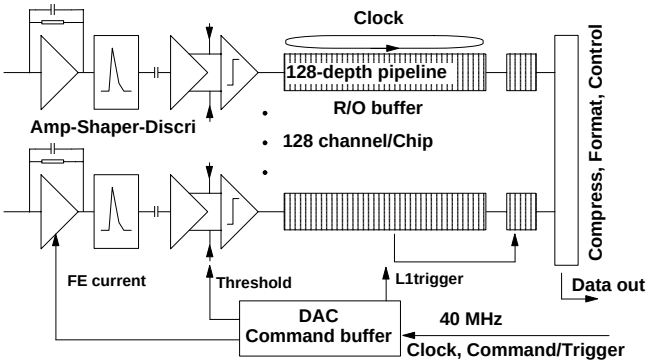

Figure 6: Schematics of the functionality of the front-end electronics

The former part of amplification in high speed is best suited for Bipolar technology while the latter part of the memories and controls is suited for CMOS technology. Development of radiation tolerant front-end electronics has been pursued in two paths: full functionarity in one BiCMOS process, the one-chip solution, and separated functionarity in a Bipolar and a CMOS processes, the two-chip solution. The chips in the former path is labelled as ABCD and the latter as CAFE/ABC, in the SCT col-

laboration.

In the ABCD design, after the feedback from the 1st generation chips, the threshold uniformity was improved by introducing extra voltage, 4 bit DAC channel-by-channel, to the main voltage, in order to fine-adjust the threshold. The 2nd generation chip is called as ABCD2T. An example of the threshold uniformity is shown in Figure 7 from the barrel module shown in section D. The sigma of uniformity is 3.2 mV, which is about 6% at the 1 fC threshold with the gain of about 55 mV/fC. There are a number of channels out of the uniformity band which is one of the remaining issues in the final design.

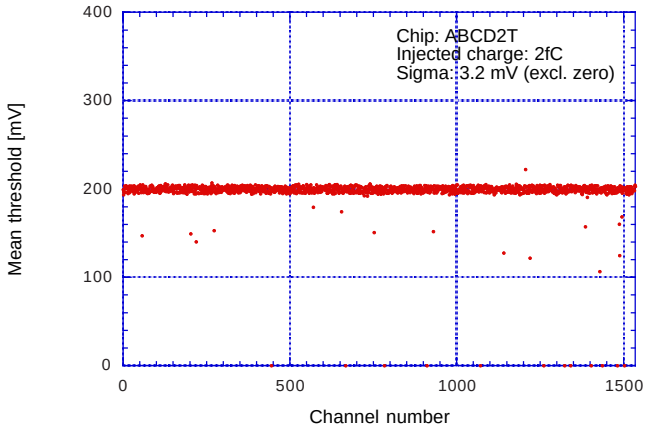

Figure 7: Uniformity of threshold in a module with 1536 channels

Radiation tolerance has been extensively evaluated: ionization damage with gamma rays of a dose of 10 Mrad and non-ionization damage with 1 MeV-equivalent neutrons of a fluence of $2x10^{14}$ n/cm^2, which is done with 24 GeV protons of $3x10^{14}$ p/cm^2 and 10 MeV neutrons from a reactor of $2x10^{14}$ n/cm^2. The major radiation damages in the chips are: degradation of beta in Bipolar-Junction-Transistors, V_t shift in MOSFET's, and increase of resistance in resistors. Results are that ABCD2T and CAFE chips almost met requirement, and still being evaluated whether all requirements are fully met, such as noise, channel-to-channel matching, time-walk, etc. Studies with more statistics are also under way.

D. SCT Silicon strip barrel module

An unit of Silicon microstrip sensors and the front-end electronics is called the module. The basic construction of the module of the barrel section is shown in Figure 8. Two 6.4 cm square sensors are aligned to form a 12 cm strip unit. The pair is aligned and glued on the top and the bottom of the central core, the baseboard, at an angle of 40 mrad to make a stereo measurement in the module.

The baseboard acts as a mechanical core and also to transfer the heat of the front-end electronics and the sensors to the cooling pipe touched at the cooling-end of the baseboard. A good heat transferring capability is critical in order prevent the thermal runaway in the sensors. The baseboard is also used as a conductor to provide a bias voltage to the backplane of the sensors. The choice of the material for the baseboard is a Carbon material called TPG which has a very good thermal conductivity of 1700 W/m/K in plane [7].

The hybrids which carry the front-end electronics are set near the centre of the module. The top and the bottom hybrids are connected at the far-end with a wrap-around inter-connection and connected to the external world through the inter-connection at the cooling end. Although not too visible in the figure, an unique feature of the module is that the hybrid has a steps at end and is bridging over the sensors; the hybrid is not glued on the surface of sensors. Electrical connections between the sensors and between the sensors and the hybrids are done with Aluminium-wire bonding. The concept of the construction of the forward modules is the similar, but the hybrid is set at the end of the module and cooling contact in the middle of hybrid to match the constraints in the disk geometry.

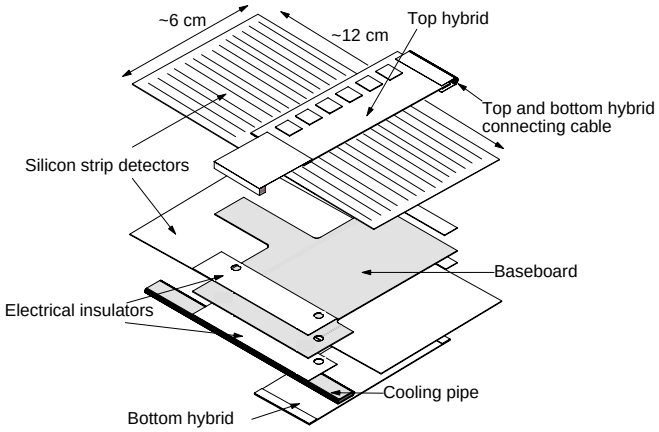

Figure 8: Construction of the barrel module

A full module has been fabricated, using ATLAS specification Silicon microstrip sensors, ABCD2T chips and a Kapton hybrid. The Kapton hybrid is a four layer lamination of Copper and Polyimide films, which allows one-piece construction of hybrids and cables, thus eliminating vulnerable connections and assuring good continuity of conductors between hybrids and cables. The fabricated modules is shown in Figure 9, in an Aluminium frame and connected to a communication card for testing. The module, although not irradiated, shows a good performance, the uniformity of threshold as shown in Figure 7, and stable operation down to the maximum of the pedestal noises.

In designing the module, major issues are three stabilities: electrical, mechanical, and thermal. The new is the thermal stability. In the SCT microstrip sensors, the leakage current increases several order of magnitude from the very low initial current, together with the increase of the full depletion voltage to several hundred volts, at the end of 10 years of operation, due

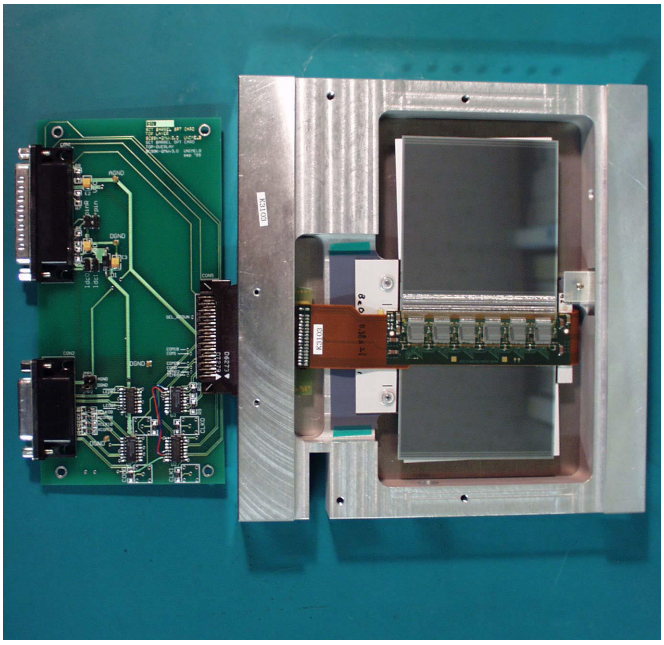

Figure 9: Fabricated barrel module being set in an Aluminium frame together with a communication card for testing

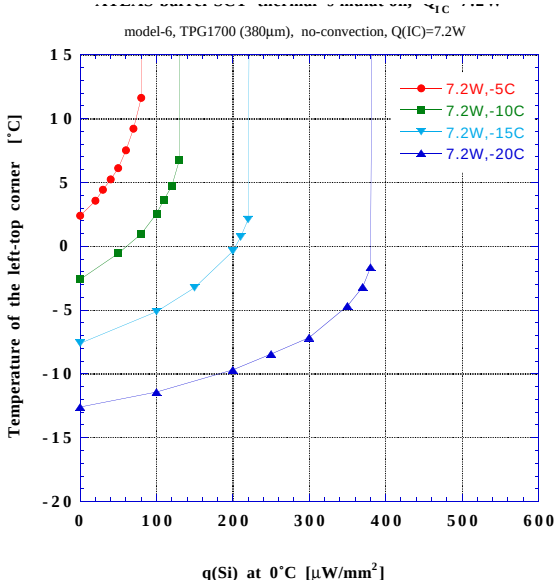

Figure 10: Thermal finite element analysis of the barrel module

to the radiation damage. The Silicon microstrip sensors are to be operated around -7 °C, in order to reduce the leakage current and to minimize the increase of full depletion voltage.

Because of the positive feedback of the temperature and the leakage current, although the module is to be operated cold, the current and the temperature will increase rapidly into the so-called thermal runaway unless cooled below a critical temperature. A thermal finite element analysis (FEA) has been made to the barrel module. The hottest temperature in the sensors are shown as a function of the heat flux, normalized at 0 °C, in Figure 10, parameterized for several coolant temperatures.

Thermal runaway occurs when the temperature is about 10 °C higher than that of the null heat flux in the sensor. The heat flux required to raise the temperature by 10 °C depends on the coolant temperature. The nominal heat flux normalized at 0 °C is about 100 µW/mm^2 at a bias voltage of 350 V. In order to expel the thermal runaway above 200 µW/mm^2, the coolant temperature must be below -15 °C.

The number of modules required in the SCT is summarized in Table 3. The SCT system is made of 4088 modules in total, 2112 modules in the barrel and 1976 modules in the forward section. A 10% of spare modules are to be fabricated, in addition. Production of the modules is scheduled to start in 2001 and complete in 2 years, at 4 assembly sites in the barrel and 3 in the forward sections. The production speed would be about 8 modules per week per site to meet the schedule.

Table 3
Number of modules in the SCT

Barrel		2112
Layer	Radius [mm]	Modules
B1	300	384
B2	373	480
B3	447	576
B4	520	672
Forward+Backward		1976
Disk	Z [mm]	Modules
D1	835	264
D2	925	184
D3	1072	264
D4	1260	264
D5	1460	264
D6	1695	264
D7	2135	184
D8	2528	184
D9	2778	104
Total		4088

E. Barrel cylinder assembly

The fabricated modules are to be positioned precisely on the cylinders in the barrel and on the disks in the forward sections. A graphical view of a barrel cylinder (B1) is shown in Figure 11 by encoding the geometry in the Geant4 program [8]. In order to prevent a hole in detecting the particles from the interaction point, adjacent modules are overlapped about 500 µm in each

end. The adjacent modules in a row are staggered with a separation of 1 mm in radius. The modules are tilted at 10° to allow overlaps in the adjacent rows.

Since the clearance between the modules is tight and the number of modules is large, a module-mounting robot is being developed. Photo's of the robot and the robot in action are shown in Figure 12. The function of the robot is not only carrying the modules into the final positions targeted by CCD cameras but also placing and tightening the dowel screws with a predetermined torque. The robot is made of 6 linear motions, 2 rotations, and 4 pressure-driven strokes. Two linear motions and one rotation are programmed to move simultaneously, 3-axis motion, in order to carry the module into the final position precisely.

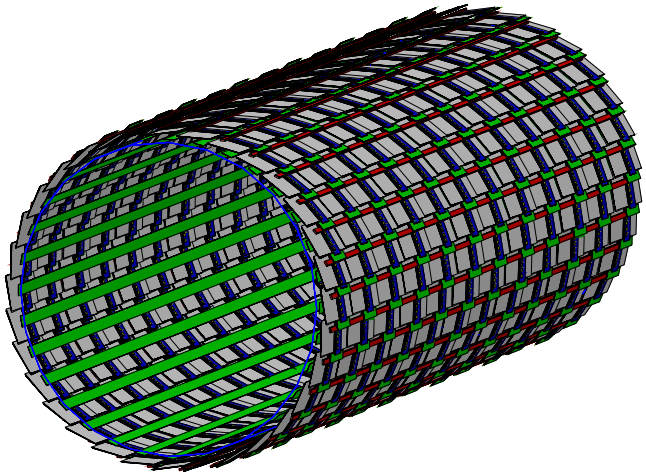

Figure 11: A graphical view of the barrel cylinder (B1). The carbon-fibre support cylinder is shown as a circle in an end.

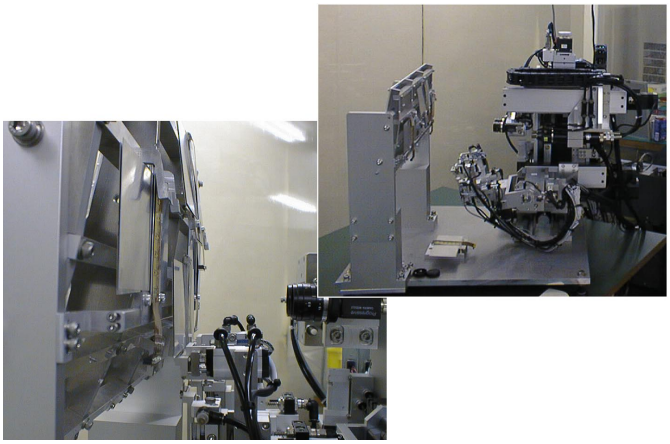

Figure 12: Module-mounting robot for the barrel cylinder. Top inset: overview together with a section of a dummy cylinder for development, and the bottom inset: the robot in action, holding a dummy module and moving toward the final position.

F. Schedule

The construction schedule of the SCT, as of November 1999, is shown in Figure 13. In order to meet the turn-on of the ATLAS detector in 2005, the installation of the inner detector is scheduled in the summer of 2004, and the installation of the SCT into the inner detector is in the spring of the same year.

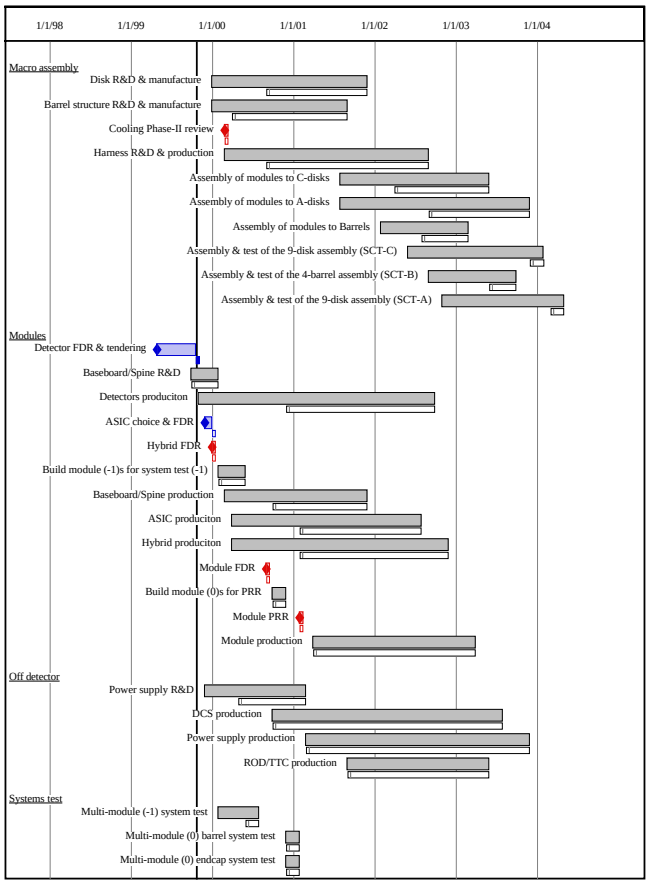

Figure 13: Construction schedule of the SCT, as of November 1999. The date in the top row is in day/month/year.

Major items of the construction of the SCT are grouped in four categories: Macro assembly, Modules, Off-detector, and System test. In the macro assembly, installation of modules on the cylinders and disks is scheduled to begin in the fall of 2001 and complete by the fall of 2003. In the fabrication of modules, pre-production of Silicon microstrip sensors starts in the end of 1999, the series production in the fall of 2000, and complete by the fall of 2002. IC's of the front-end electronics is following the sensor production but completing earlier. Module assembly is following the series production of sensors and IC's and completing by the spring of 2003. The verification of the SCT with prototype setups, the system tests, are scheduled in 2000 in order to start the above construction in the beginning of 2001.

IV. Summary

ATLAS detector, exploring physics of Higgs particles and

others in TeV energy region, is under construction. One of the precision charged particle tracking devices near the interaction point inside a solenoidal magnetic field is the SCT, based on the Silicon microstrip sensor technology. Understanding and development in Silicon microstrip sensors have shown that the p-readout microstrip sensors in the n-bulk Silicon can survive the radiation damage of the fluence of 2 x 10^{14} 1-MeV equivalent neutrons/cm^2.

The front-end electronics is on/off “binary” readout with buffering memories having stored the signals till the readout trigger comes. Three types of radiation-hard LSIs are under development: full functionarity in one chip, ABCD by BiCMOS rad-hard process; analog functionarity in one chip, CAFE by Bipolar, and a digital functionarity in the other chip, ABC by CMOS rad-hard processes. Although still more work is required, all the chips have come to the level fulfilling the most of the requirements, including radiation tolerance.

A fully loaded module of the barrel section, with the ATLAS specification Silicon microstrip sensors and the latest ABCD chip, ABCD2T, has been built and shown a successful stable operation.

The SCT is in it’s final design phase and moving rapidly to the construction by 2001. A total of 19500 Silicon microstrip sensors are to be produced in 3 years and 4500 modules in 2 years. The SCT will be completed and installed by the spring of 2004, and the ATLAS will be ready for experiment in the middle of 2005.

V. References

[1] The LHC Conceptual Design Report - The Yellow Book, CERN/AC/95-05(LHC) (1995)

[2] ATLAS Technical Proposal for a General-Purpose pp Experiment at the Large Hadron Collider at CERN, CERN/LHCC/94-43 (1994)

[3] E.g., ATLAS Inner Detector Technical Design Report Vol. 1, ATLAS TDR 4, CERN/LHCC 97-16 (1997); Vol. 2, ATLAS TDR 5, CERN/LHCC 97-17 (1997)

[4] Fabricated by Hamamatsu Photonics Co. Ltd., Ichino, Hamamatsu 435-8558, Japan

[5] H.-J. Ziock et al., Nucl. Instr. Meth. A342 (1994) 96-104

[6] T. Ohsugi et al., Nucl. Instr. Meth. A342 (1994) 22-26

[7] Thermal Pyrolytic Graphite made by Advanced Ceramics Corporation, P.O.Box 94924, Cleveland, Ohio 44101, U.S.A.

[8] Geant4, a tool kit for the simulation of the passage of particles through matter, http://wwwinfo.cern.ch/asd/geant4/geant4.html